A novel optimisation process for static structural finite element analysis of offshore wind turbine floating foundations

Proceedings of the Thirty-fourth (2024) International Ocean and Polar Engineering Conference **www.isope.org**
Rhodes, Greece, June 16–21, 2024

ISBN 978-1-880653-78-4; ISSN 1098-6189

A novel optimisation process for static structural finite element analysis of offshore wind turbine floating foundations

Massimo Sirigu, Alberto Ghigo, Giuseppe Giorgi and Giovanni Bracco
Marine Offshore Renewable Energy Lab (MOREnergy Lab),
Department of Mechanical and Aerospace Engineering (DIMEAS),
Politecnico di Torino, Turin, Italy

ABSTRACT

The study presents a novel optimisation process for structural finite element analysis for a floating foundation for offshore wind turbines. The methodology is based on Ansys Pymechanical scripting for a semisubmersible platform. The structural analysis includes hydrostatic pressure, static aerodynamic thrust and turbine weight, and mooring loads. The optimisation is single objective, aiming to reduce mass and constrained by yield stress and buckling instability. The results show the capabilities of the methodology to achieve an optimal configuration of thicknesses and dimension of internal stiffeners.

KEY WORDS: Finite element analysis; structural mechanics; floating offshore wind turbines: structural optimisation

INTRODUCTION

There is a growing emphasis on developing cost-effective floating wind turbines, which necessitates the use of efficient stress analysis methods for the structural design of platforms. Most existing studies primarily employ global analysis methods, treating the platform as a rigid body, and as a result, they do not directly provide insights into the stress distribution within the substructure. The research in this field is also limited by the lack of publicly accessible references for the internal specifications of stiffeners and plate thicknesses.

The present literature review shows an overview of the current state of the art in the structural analysis of floating substructures, focusing on recent advancements and key findings in this field; in (Ivanov, Hsu, and Ma 2023), the paper studies and compares different shapes of a floater for a 15 MW wind turbine. Key findings of the paper are that bracing is important to correctly withstand the wind turbine loads. An uneven hexahedral column shape is suggested as a superior alternative to cylindrical columns, combining ease of manufacture with low drag.

In another significant contribution, (Park and Choung 2023) utilises dominant load parameters (DLPs) like acceleration and nacelle thrust, considering the extreme conditions of a 50-year return period. A comprehensive assessment includes frequency response hydrodynamic analysis, finite element modelling, and long-term load analysis. The findings reveal the significance of the DLP in assessing the substructure strength of FOWTs, highlighting areas where stresses exceed permissible levels and suggesting structural reinforcements.

The paper (Starr et al. 2017) presents a comparison of different methods for structural analysis of a Tension Leg Platform (TLP), made of simple tubular elements. The paper emphasizes the effectiveness of the sub-modelling technique in structural analysis. It compares well with methods using locally applied sectional loads, especially when stiffness representations are identical. However, local loads significantly affect the support structure, not accounted for in the global shell model, leading to slightly lower stress results.

Other papers (Vasconcelos et al. 2020; Hussein et al. 2013) focus on a parametric study of the examined platform, respectively the Three-Column platform, as the WindFloat concept, and the semisubmersible DeepCwind reference platform.

Existing literature predominantly focuses on comparative analyses of platform shapes or conducts parametric studies on variables like thickness and number of stiffeners. These approaches, while informative, often result in designs that are suboptimal in terms of material usage. A recurring observation is the excessive use of structural steel compared to estimates derived from reference models. This discrepancy not only indicates potential inefficiencies but also underscores a gap in the field: the absence of a systematic process for structural optimisation of floaters.

Addressing this gap, our study introduces a novel methodology for the structural optimisation of floating platforms. Unlike previous studies, our approach explicitly targets the reduction of steel mass while ensuring the maintenance of key structural integrity parameters, namely yield stress and linear buckling strength. This dual focus is essential for enhancing the reliability and safety of these structures.

The selected structure for analysis is the Volturn US platform (Allen et al. 2020), which mounts the IEA 15MW reference wind turbine (Gaertner et al. 2020).

In order to determine the optimal design of the platform, a static structural optimisation process is performed. The process employs Ansys Pymechanical scripting, facilitating finite element analysis through Ansys Mechanical 2023R1.

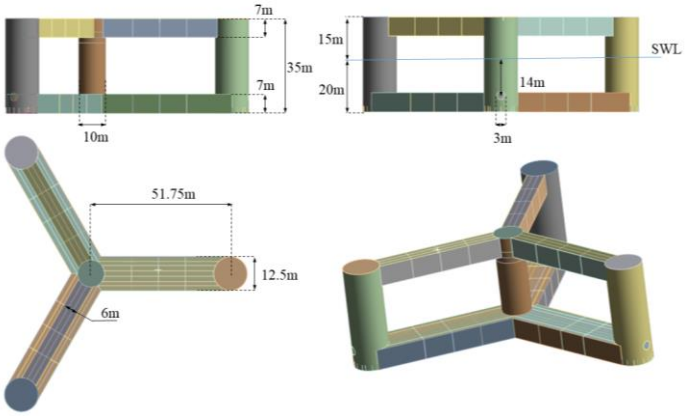

Fig. 1: Definition of external geometry of the floater (Allen et al. 2020).

The focus of this methodology lies in dividing the optimisation process into sub-optimisations, varying the thicknesses of groups of shells, while the location and dimensions of the internal reinforcements are manually set after the results of the sub-optimisation on the weak points. It adopts a single-objective optimisation approach, aiming to minimize the structural steel mass. It is important to note that the external geometry, which defines attributes such as submerged volume, hydrostatic stiffness, and centre of buoyancy, is fixed throughout all the optimisation steps.

STATIC STRUCTURAL IMPLEMENTATION

Ansys model

The analysis includes a variety of static loads that the structure must endure. These loads include:

1. Hydrostatic pressure from sea water.
2. Forces and moments resulting from static aerodynamic thrust and the weight of the turbine.
3. Loads from the mooring lines.
4. Hydrostatic pressure from internal ballast.

For calculating the loads transferred by the tower and the mooring lines, OpenFAST ("OpenFAST" 2024), an open-source software developed for the dynamic analysis of floating wind turbines, is employed.

Fig. 1 displays the platform's external dimensions. In comparison to the reference model cited in (Allen et al. 2020), the original tubular braces have been replaced with larger, square braces. the new braces measure 6 meters wide and 7 meters tall, a change made to improve the platform's structural strength. Since the braces are located above the sea water level (SWL), this change does not impact the hydrostatic and hydrodynamic behaviour of the substructure.

The platform's geometric design is carried out using Salome 9.9.0 ("Salome 9.9.0" 2024), an open-source software for 3D CAD modelling. To fuse together the surfaces created by Salome (.iges format), Ansys Spaceclaim is used. Without this step, each surface is treated separately by Ansys Mechanical.

To maintain the required draft from design, a specific quantity of ballast is necessary. The mass of structural steel used in the platform is determined after setting the thickness for each designated group of shell elements. The calculation for the required ballast is explained in Eq. 1, Where ρ is the density of sea water (1025 kg m^{-3}), V_s is the submerged volume (20206 m^3), $M_{waterBallast}$ is the water ballast contained in the pontoons (11554 ton), $M_{turbine}$ is the mass of the wind turbine (2425 ton) and M_{steel} is the structural mass, $F_{preload}$ is the mooring preload (6.26 MN) divided by the gravity acceleration.

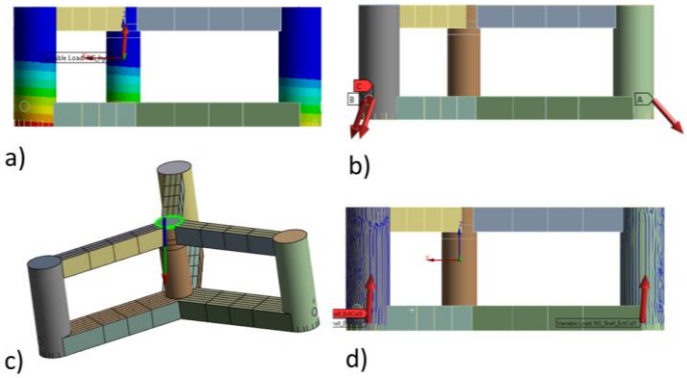

Fig. 2: Representation of external loads in Ansys. a) Distribution of hydrostatic pressure. b) Mooring forces at fairleads. c) Reaction force of fixed constraint at tower base. d) Internal hydrostatic pressure of ballast.

$$M_{ballast} = \rho \cdot V_s - M_{steel} - M_{waterBallast} - M_{turbine} - \frac{F_{preload}}{g} \quad (1)$$

The centre of mass of the platform is then evaluated by summing the centre of mass (CoM) of steel, the centre of mass of water ballast in the pontoons and additional ballast and dividing the result by the total mass, assuming that the ballast density is 2200 kg m^{-3} (generic concrete ballast), and the ballast is located at the bottom of the external columns. The ballast is represented as an internal hydrostatic pressure. This internal pressure is advantageous for the structural integrity of the platform because it counteracts the external hydrostatic pressure exerted by seawater. The level of this internal pressure corresponds to the height of the ballast. Additionally, the model includes the gravitational force resulting from the mass of the steel.

The pontoons in the design do not experience hydrostatic pressure due to the presence of water ballast within them. It is assumed that there is a balance between the internal and external pressures, allowed by a possible (small) mass exchange between the inside and outside of the pontoons, thereby equalizing the pressures (Fig. 2).

If the pontoons are assumed completely sealed (for example, considering a transportation without internal ballast to achieve lower draft in the port), the hydrostatic pressure would be function of the deformed volume of the pontoons. This fact would require a finite element analysis considering deformation under external loads and the increased pressure derived from the compressibility of the fluid ballast.

To prevent the rigid body motion, two types of constraint methods were explored: inertial relief and a fixed constraint at the interface between the tower and the platform.

Inertial relief is a technique that counteracts unbalanced forces by applying acceleration forces to the mass elements. This method effectively counteracts any small resultant forces that could cause movement. It's crucial that the resultant acceleration is minimal, only sufficient to offset any imperfections in force application. Given these premises, inertial relief may be considered the best choice to represent the floater's constraints, as it avoids issues of over-constraining.

However, in Ansys mechanical it is not possible to perform eigenvalue buckling analyses using the pre-stress distribution created by inertial relief. Due to this limitation, a fixed constraint was ultimately implemented around the circumference of the tower-platform interface, as shown in Fig. 2. This fixed constraint method can have some issues: it could distort the real stress distribution because the base of the tower is treated as non-deformable. Therefore, it is important to be cautious and ensure this approach does not create artificial stress concentrations

around this area.
To factor in the aerodynamic thrust forces and moments, as well as the self-weight of the wind turbine, the platform's orientation is adjusted relative to the sea water level (SWL). These specific values are derived from time-domain simulations conducted in the OpenFAST model.
The distribution of hydrostatic pressure, altered by the pitch and roll angles and heave, predominantly determines the tower's reaction forces. These forces are crucial as they support the weight of the turbine and counterbalance the pitching and rolling moments caused by turbine thrust. In other terms, instead of directly evaluating the forces on the tower base from actual thrust and weight, these forces are evaluated from the reaction forces obtained from the distribution of hydrostatic pressure and mooring lines, and then compared with OpenFAST tower base internal forces and moments.
The mooring loads are applied as forces distributed over the surface of the fairleads. Each fairlead is modelled as a circular area on the external columns with a diameter of 3 meters.
For clarity purposes, the process followed in the Ansys model can be outlined in steps described in Tab. 1. The computational time expressed in Tab. 1 are indicative for a medium-performance laptop.

Tab. 1: definition of steps of global workflow and relative computational time. In light red, steps computed before the optimisation. In light green, steps carried out during each step of the optimisation.

Step	Process	Time
1	Creation of .iges files in Salome	5 s
2	Use of Ansys Spaceclaim to fuse surfaces together	30 s
3	The geometry is loaded into Ansys.	30 s
4	Structure is meshed.	25 s
5	The thicknesses for groups of surfaces are set.	-
6	The total mass of structural steel is calculated.	-
7	The ballast required for the platform is computed.	-
8	The centre of mass (CoM) of the platform, including structural steel and ballast, is determined.	-
9	Values for pitch, roll, heave, and mooring forces are interpolated based on the CoM using results in OpenFAST.	-
10	The static structural analysis is performed.	20 s
11	The eigenvalue buckling analysis is performed.	20 s

OpenFAST model

The OpenFAST model evaluates the heave, pitch, and roll angles, which are necessary to model the hydrostatic pressure distribution and the mooring forces acting on the fairleads. Additionally, it evaluates and the forces and moments at the tower base for comparison purposes.
Simulations of 400 seconds are conducted with additional linear damping, aiming to achieve steady-state values. These simulations take place under still water conditions and a constant wind speed corresponding to the rated wind speed of 10.56 m/s. The process involves conducting several simulations with different centre of mass (CoM) values for the platform. The outcomes of these simulations are analysed using linear interpolation, as the relationships between the variables and the platform's CoM are predominantly linear, with a weak non-linearity due to the mooring system. This analysis uses four CoM values, ranging from -13 to -16 meters below sea water level.
The equations for the interpolation of these key values are presented for reference (Eq. 2 and 3). The mooring forces are then rotated from the global reference system of the SWL to the local reference system of the platform.

$$\begin{cases} \text{pitch} = 0.20\ \text{CoM} + 6.610 \\ \text{heave} = -0.00122\ \text{CoM} - 0.0727 \\ \text{roll} = 0.023\ \text{CoM} + 0.764 \end{cases} \quad (2)$$

$$\begin{cases} F_{\text{moorX1}} = -2130\ \text{CoM} + 2742236 \\ F_{\text{moorX2}} = -2.76\ \text{CoM} - 480820 \\ F_{\text{moorX3}} = -224.1\ \text{CoM} - 481744 \\ F_{\text{moorY1}} = 7.44\ \text{CoM} - 0.777 \\ F_{\text{moorY2}} = 354.2\ \text{CoM} - 865322 \\ F_{\text{moorY3}} = 205.4\ \text{CoM} + 870768 \\ F_{\text{moorZ1}} = 828.1\ \text{CoM} + 2726231 \\ F_{\text{moorZ2}} = -702.2\ \text{CoM} + 1807237 \\ F_{\text{moorZ3}} = -626.1\ \text{CoM} + 1801219 \end{cases} \quad (3)$$

OPTIMISATION PROCESS

Optimisation definition

The optimisation process utilized in this study employs the "scipy.optimize.fmin" function from the SciPy library ("Fmin Function" 2024). This function implements the Nelder-Mead algorithm, which is a derivative-free optimiser designed to locate the local minimum of a given function. The choice of this algorithm was driven by its straightforward implementation and its ability to rapidly converge to a solution. However, it is acknowledged that the Nelder-Mead algorithm may not be the most effective approach for larger-scale problems characterized by a high number of input variables, the presence of multiple local minima and dependency on the starting point. Future research can benefit by the transition from the local optimiser to a global optimisation strategy, potentially employing methodologies like particle swarm optimisation or genetic algorithms.

Optimisation workflow

The "fmin" function in our optimisation process is configured to modify the thicknesses of various structural components, such as the main column, external columns, and internal stiffeners. The location and dimensions of the stiffeners are chosen manually before the optimisation. We have chosen not to alter the locations of the internal stiffeners during the optimisation to achieve two primary objectives: firstly, this approach helps in restricting the number of input variables, which, in our study, is limited to between 4 and 11. Secondly, by maintaining a consistent geometry and mesh across all iterations, we significantly streamline the workflow. Keeping in mind the steps expressed in Tab. 1, this methodology enables us to start the optimisation from step 5 (setting up thicknesses) and proceed until to the step 11 (buckling analysis), highlighted in light green.
This efficiency gain is particularly significant compared to a workflow that would involve starting anew with a fresh geometry in Salome, followed by the geometry import and meshing. In such a way, the computational time is reduced by 2-3 times.

Objective function and constraints definition

The goal of the optimisation process is to minimize the total mass of structural steel, while also integrating the constraints into the model. These constraints include two main types: yield stress and buckling strength.
The first one involves the evaluation of Von Mises stress computed at at the shell element centroid of the mid-plane (DNVGL-CG-0127), to be compared to the yield stress of steel, that in our case is 355 MPa. This value is often used for offshore wind platforms (Park and Choung 2023; Vasconcelos et al. 2020).
(DNV-ST-0119) introduces two safety factors: one for loads and one for materials. For the loads, DLC 1.1 (power production) related safety factor is used, that corresponds to 1.25, as stated in (DNVGL-ST-0437). The material safety factor is 1.1 for ULS for welded structural plates (DNV-ST-0119).
We have used an increased safety factor of 1.5, and the limit for the stress

results in 235 MPa.
Eigenvalue buckling analysis involves solving an eigenvalue problem derived from the equilibrium equations of a structure. In this context, an eigenvalue is a scalar factor, also called load multiplier, that, when multiplied by a certain load, leads to a state where the structure loses its stiffness and stability. This analysis is particularly important for floating wind platforms, as they are predominantly made up of shell elements under compressive stress, making them highly susceptible to buckling instabilities. From DNV standards (DNVGL-ST-0437), when using EN 1993-1-6 standard, material buckling safety factor for shells is 1.1 (load safety factor remains 1.25). For this structure, the safety factor applied to the load multiplier for the first mode of buckling is set at 1.5.
Note that the DNV safety factors relate to time-domain results in respect of transient effects of waves and wind turbulence. In our case, the loads were meant for the design optimization and, hence, do not present themselves as design load cases according to the standards. In any case, a first design would be useful for implementation of real conditions of the platform.
The objective function in the optimisation integrates these two kinds of constraints as penalties, along with the assessment of steel mass. These penalties are structured as parabolic functions based on the specific constraint being considered. The objective function is outlined in Eq. 4, 5 and 6, Where σ is the Von Mises stress and LM is the load multiplier of the first mode of buckling.

$$OBJ = M_{steel} + OBJ_{Yield} + OBJ_{buck} \tag{4}$$

$$\begin{cases} OBJ_{Yield} = 0.4\,\sigma^2 - 112\,\sigma + 9000, & if\ \sigma > 235 \\ OBJ_{Yield} = 0, & if\ \sigma < 235 \end{cases} \tag{5}$$

$$\begin{cases} OBJ_{Buck} = 16032\,LM^2 - 48080\,LM + 36048, & if\ LM < 1.5 \\ OBJ_{Buck} = 0, & if\ LM > 1.5 \end{cases} \tag{6}$$

RESULTS

First attempt

The optimisation process begins by focusing on the structure's external geometry, which consists of shell elements. Internally, the only components considered are the walls that separate the cylinders from the pontoons and braces, as well as the connectors linking the pontoons. This initial configuration is illustrated in Fig. 3.
In this stage, the thickness of the structural elements is categorized and set for four distinct groups: the external columns, the main column, the pontoons, and the braces.
For a global analysis with coarse mesh, as stated in (DNVGL-CG-0127), the size of the mesh must be SxS, where S is the stiffeners' spacing. In our model, we used a mesh size of 1 metre, avoiding capturing concentration stresses at connections. Finer mesh should be implemented for partial and local structural analyses. While 1 metre represents a relatively coarse mesh, it is intentionally chosen to enable the rapid evaluation of a large number of structural combinations. This approach is beneficial in terms of computational efficiency, as it keeps the time required for each function evaluation within a manageable range of 30 to 40 seconds.
The initial thicknesses of the external columns, the main column, and the pontoon are each set at 5 centimetres. For the braces, a slightly thinner dimension of 3 centimetres is chosen.
Figure 4 presents a graphical representation of how certain key factors evolve during the optimisation process. These factors include the total mass of steel used in the structure, the constraints, and the inputs applied at each step of the process.
The optimisation algorithm reached a point of convergence after approximately 250 iterations.
The results indicate that the total weight of the platform is greater than the allowable steel mass. This maximum allowable steel mass is 6089 tons, which is the steel mass when it carries no ballast mass, as determined by Eq. 1. This implies that the platform cannot achieve the necessary draft as specified by the design requirements.
As a result of this issue, the stress patterns observed on the platform do not accurately represent the realistic stress conditions. This inaccuracy stems from the observed forces at the tower's fixed constraints, which are lower than expected or even positive. This suggests that the platform, in its current state, cannot maintain the floating condition, even without the additional weight of the turbine.
Figure 5 shows the distribution of stress on the optimised platform. This stress map highlights that the bottoms of the cylindrical columns are critical areas in terms of design. These areas require a substantial increase in material thickness to withstand deformation — specifically, 14 cm for external columns and 10 cm for the main column.

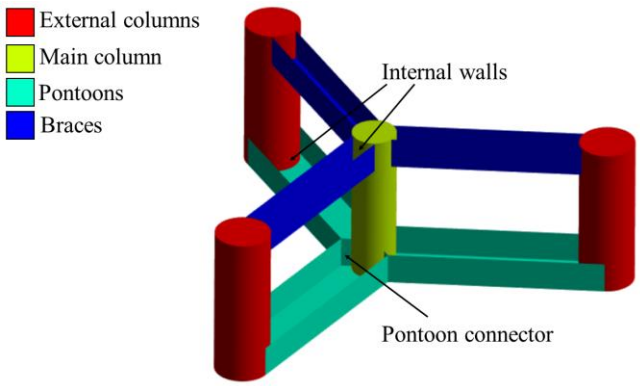

Fig. 3: Definition of group of surfaces to set the thicknesses for the first optimisation attempt.

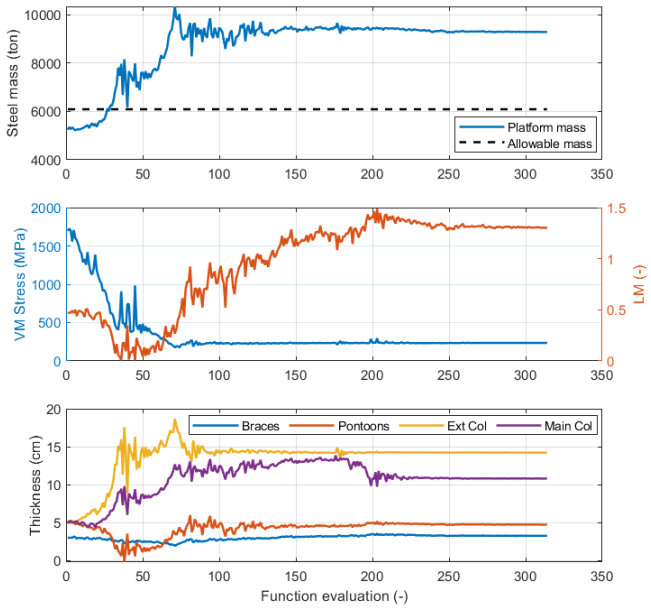

Fig. 4: Results from "fmin" iterations for steel mass, Von Mises Stress, load multiplier, and thicknesses of surface groups.

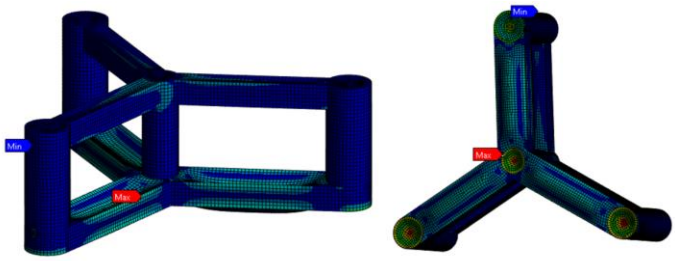

Fig. 5: Stress distribution of the platform after first attempt of optimisation

In response to these insights, a second iteration of design optimisation is undertaken. This iteration involves adding reinforcements and adjusting the thicknesses of various structural elements to address the identified weaknesses. The platform is then re-optimised based on these new specifications.

Second attempt

In the second optimisation attempt, additional stiffeners are introduced to the main and external columns of the structure. These stiffeners are specifically designed to counteract the hydrostatic pressure at the bottom of the columns. Fig. 11 illustrates these stiffeners, which are arranged to form a square grid pattern. Each stiffener has a height of 2 meters. The external columns are equipped with 5 stiffeners each, while the main column has 4 stiffeners. To facilitate this optimisation, two new variables are introduced: the thickness of the stiffeners on the external columns and the thickness of those on the main column.

The progress of this optimisation is charted in Fig. 6. The addition of these new stiffeners significantly reduced the thickness required for the columns. This led to a substantial reduction in the overall mass of the platform, bringing it down from 9322 tons to 6357 tons, which is about a one third decrease.

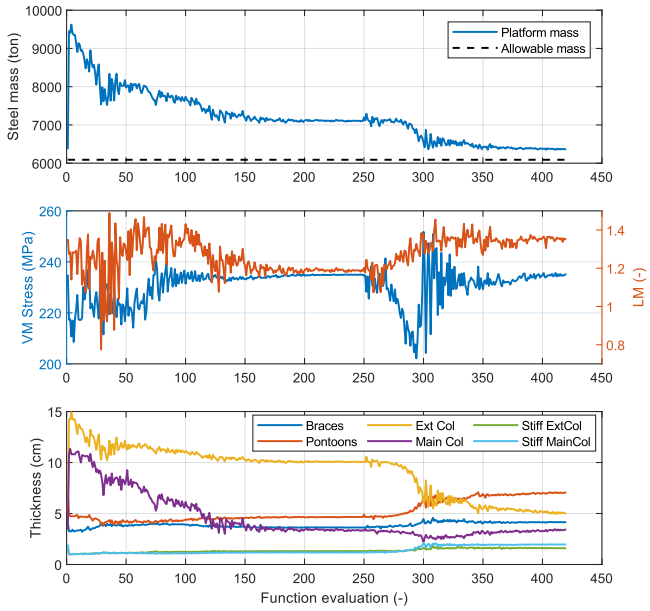

Fig 6: Results from second attempt of optimisation, including stiffeners of external and main columns.

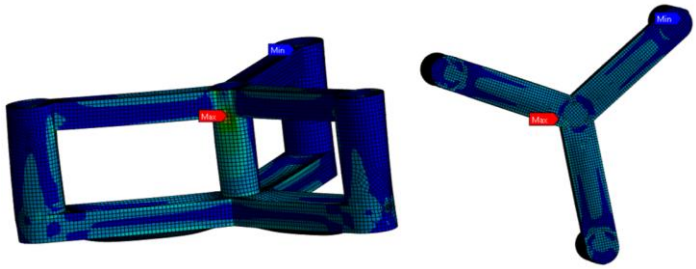

Fig7: Stress distribution of platform after the second attempt of optimisation, including stiffeners at bottom of the columns.

At the 251st iteration, the optimisation algorithm "fmin" was restarted. This restart is evident in Fig. 6 as a perturbation in the data. This step was necessary to move the optimisation process out of a local minimum where it had become stuck. This situation highlights a common issue with the gradient-based algorithm, namely its difficulty in consistently converging to a global minimum. Fig. 7 displays the distribution of stress in the newly optimised structure. The stress is now primarily concentrated in the arms and at the junctions where the braces connect to the main column. The pontoon thickness is now 7 cm. Given these observations, there is potential for further optimisation of the pontoons, possibly by adding new stiffeners to these components.

New attempts

New modifications to the design introduce additional support structures at various points of the structure. This includes the stiffeners and girders on the pontoons and the braces, and the radial rings within the main column. Due to space limitations, this section provides a global overview of these enhancements.

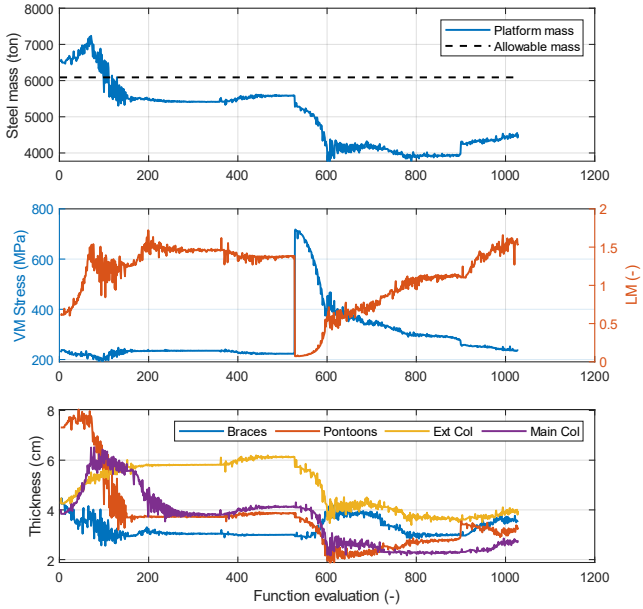

Fig. 8: summary of the optimisation with new internal reinforcements: internal stiffeners on the pontoons and braces and radial stiffeners inside the main column. Only the thicknesses of main geometries are shown in figure for space limitations.

These new elements were incorporated in a sequential manner. Initially, the girders were added to the pontoons and braces from the first iteration. Subsequently, in iteration 72, longitudinal stiffeners were introduced to the arms and pontoons. Finally, in iteration 528, radial stiffeners were installed inside the main column.
For a detailed understanding of the dimensions and specifications of these new elements, please refer to the subsection titled “Final design definition”.
As clearly illustrated in Fig. 8, the integration of these elements has successfully led to a feasible design. The inclusion of girders and longitudinal stiffeners resulted in the platform's weight reaching approximately 5600 tons. Additionally, there was a reduction in the thickness of the pontoons from 7 cm to 3.2 cm. The longitudinal stiffeners measure 1.16 cm in thickness, and the girders are 0.93 cm thick. It was observed that the girders alone were not enough to reduce stress.
The further addition of radial rings proved to be highly effective. These stiffeners significantly contributed to managing the stress concentration at the junctions where the main column connects to the braces. This modification reduced the overall mass of the structure from 5600 tons to 4500 tons.
It is noteworthy to say that the thickness of the radial stiffeners (80.6 mm) appears to be too large for manufacturing, but a new optimisation with more than three radial stiffeners can be placed for future work. Also, the external columns can benefit from the introduction of internal stiffeners to limit the thickness (now 39.7 mm).
Fig. 9 showcases the distribution of mechanical stress across the final design of the platform. While this version shows some minor areas of local stress concentration, this platform could be the starting point of future optimisation efforts. The primary points of maximum stress are identified at the junctions of the pontoons and braces.

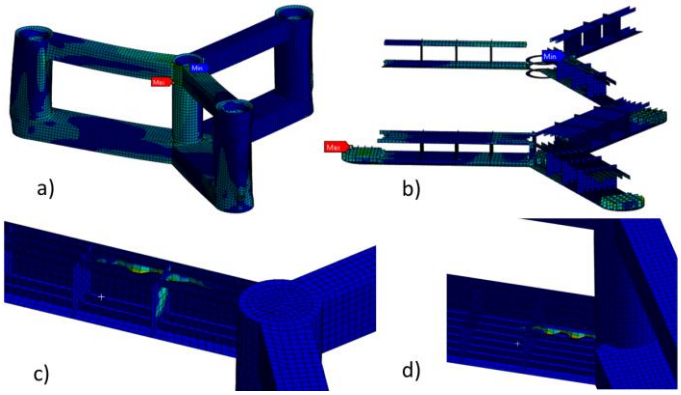

Fig. 9: results from Ansys of optimal geometry. a) Stress field on external geometry. b) Stress field on internal reinforcements. c) First mode of buckling (brace and girder stiffener). d) Second mode of buckling (pontoon stiffener).

Tab.2: comparison of reaction forces at fixed constraint between Ansys mechanical and OpenFAST

Tower reaction forces and moments	Ansys results	Error respect to OpenFAST results
Fx	3.308 MN	0.19 %
Fy	-0.2258 MN	0.41 %
Fz	-23.496 MN	-1.01 %
Mx	31.096 MNm	0.81 %
My	298.84 MNm	0.16 %
Mz	-0.1726 MNm	0.34 %

Reducing the stress at the pontoons junction might be achievable by designing a specialized fitting for that connection.
The first buckling mode occurs in the longitudinal stiffeners and girder of the brace, while the second buckling mode occurs in the longitudinal stiffeners of the pontoon. These modes have load multipliers of 1.588 and 1.636, respectively.
Finally, the reaction forces and moments at the tower base were compared with OpenFAST results in Tab. 2, showing that the percentage error for all forces and moments is below 1%.

Final design definition

In the present subsection, the final optimised model is described. In Fig. 9, the 10 groups of surfaces are shown. Each group share the same value of thickness.
The external geometry of this structure was previously illustrated in Fig. 1, and we will now focus on the internal geometry.
In Fig. 11, the floater's bottom plan is shown, including the dimensions of its internal stiffeners. There are 6 longitudinal stiffeners along the pontoons, extending from the main column's internal walls to the external columns and evenly spaced apart. Additionally, there are three girders, starting 15 meters from the main column's centre and spaced 10 meters apart. The stiffeners stand 1 meter tall.
Each column contains stiffeners arranged in a squared grid pattern, with a 2-meter gap between them. Specifically, the main column has four stiffeners, while the external columns each have five, all measuring 2 meters in height.
Regarding the braces, they are equipped with two stiffeners, mirroring the height and girder placement of the pontoons’ stiffeners (Fig. 12).
Within the central column, radial stiffeners with 1 meter of width are strategically placed near the junction of the main column and the braces. There are three of these, with the central stiffener located right at the bottom of the brace, and the other two spaced 2 meters apart.
The global values regarding the mass of steel, ballast, centre of mass and other variables are shown in Tab. 3.

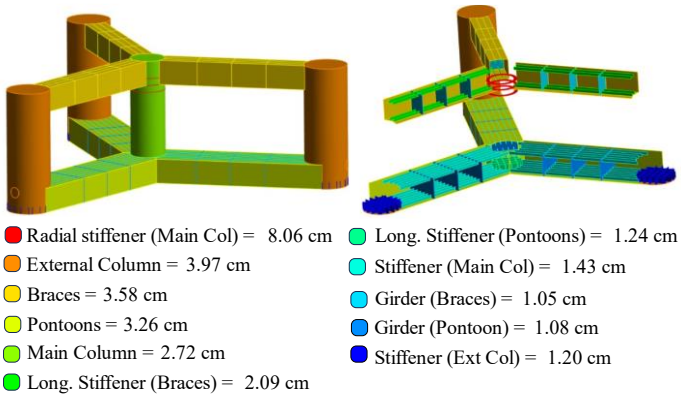

Fig.10: Definition of geometric elements with identical thickness values.

Tab. 3: final values for the optimised platform

Variable	**Value**
Structural steel mass	4515 tons
Ballast mass	1572 tons
Water ballast mass	11554 tons
Platform centre of mass	-13.93 m
Platform pitch in rated wind speed	3.82 deg
Max stress	234.2 MPa
Load multiplier for 1st mode	1.588
Load multiplier for 2nd mode	1.636

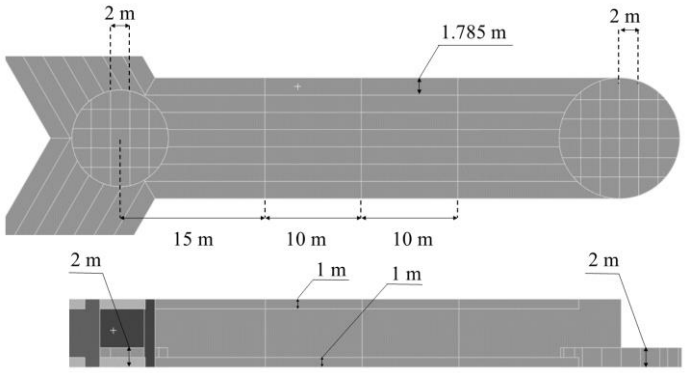

Fig. 11: Top and lateral view of pontoon and stiffeners of main and external column.

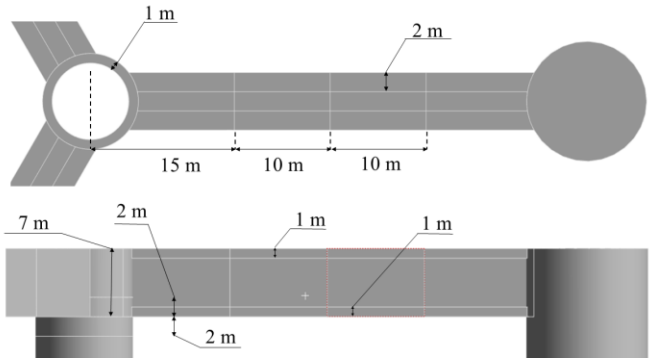

Fig. 12: Top and lateral view of brace and radial stiffeners of main column.

CONCLUSION

This paper presented a structural optimisation of a semisubmersible platform designed for offshore wind turbines, specifically the Volturn US platform for the IEA 15 MW wind turbine. Key points of the study are summarised as follows:

1. Optimisation process: the optimisation was divided into several steps. Initially, the weak points of the substructure were identified. Subsequently, additional stiffeners were manually incorporated at the weak points, and the thickness of various geometric groups was optimised to reinforce these points.
2. Achievements: the optimised platform closely matches reference steel mass values while adhering to critical constraints, such as a maximum allowable stress of 235 MPa and a buckling strength safety factor of 1.5.
3. Importance of stiffeners: the study highlights the crucial role of the placement and dimensions of internal stiffeners in reducing the overall mass, particularly in the bottom part of the columns.
4. Optimisation algorithm: a suggestion is made to replace the Nelder-Mead optimisation algorithm as the number of variables increases, to avoid the optimisation process getting trapped in local minima for example considering global optimisers like genetic algorithms or particle swarm optimisation.
5. Limitations: the research only considered static loads. It is recommended to compare these results with time-domain simulations that adhere to standard design load cases, including transient effects and wave loads.
6. Future works: different shapes or new placements of internal stiffeners can be explored, aiming not only to reduce steel mass but also to improve safety factors for yield stress and buckling strength. future considerations should also include manufacturing costs, particularly how the location and number of stiffeners impact expenses such as welding.

In conclusion, this research underscores the need for a more thorough approach in the structural analysis of floating wind turbine platforms as it provided valuable insights for optimizing structural design parameters.

REFERENCES

Allen, Christopher, Anthony Viselli, Habib Dagher Andrew Goupee, Evan Gaertner, Nikhar Abbas, Matthew Hall, and Garrett Barter. 2020. “Definition of the UMaine VolturnUS-S Reference Platform Developed for the IEA Wind 15-Megawatt Offshore Reference Wind Turbine Technical Report.” www.nrel.gov/publications.

DNVGL-CG-0127 2015. “CLASS GUIDELINE Finite Element Analysis.”

DNV-ST-0119 2016. “Loads and Site Conditions for Wind Turbines.”

DNVGL-ST-0437 2016. “Support Structures for Wind Turbines.”

“Fmin Function.” 2024. https://docs.scipy.org/doc/scipy/reference/generated/scipy.optimize.fmin.html.

Gaertner, Evan, Jennifer Rinker, Latha Sethuraman, Frederik Zahle, Benjamin Anderson, Garrett Barter, Nikhar Abbas, et al. 2020. “Definition of the IEA Wind 15-Megawatt Offshore Reference Wind Turbine Technical Report.” www.nrel.gov/publications.

Hussein, Karim R, Arwa W Hussein, El-Sayedh Hegazy, and Ahmed A Amin. 2013. “Structural Design of a Floating Foundation for Offshore Wind Turbine in Red Sea.”

Ivanov, Glib, I. Jen Hsu, and Kai Tung Ma. 2023. “Design Considerations on Semi-Submersible Columns, Bracings and Pontoons for Floating Wind.” *Journal of Marine Science and Engineering* 11 (9). https://doi.org/10.3390/jmse11091663.

“OpenFAST.” 2024. 2024. https://openfast.readthedocs.io/en/dev/source/user/general.html.

Park, Sungjun, and Joonmo Choung. 2023. “Structural Design of the Substructure of a 10 MW Floating Offshore Wind Turbine System Using Dominant Load Parameters.” *Journal of Marine Science and Engineering* 11 (5). https://doi.org/10.3390/jmse11051048.

“Salome 9.9.0.” 2024. https://www.salome-platform.org/.

Starr, Markus S, Andreas Manjock, Christian Arjes, Ngoc-Do Nguyen, and Ing Torsten Faber. 2017. “FINITE ELEMENT METHODS FOR THE STRUCTURAL ANALYSIS OF TENSION LEG PLATFORMS FOR FLOATING WIND TURBINES.” http://asmedigitalcollection.asme.org/OMAE/proceedings-pdf/OMAE2017/57663/V03BT02A038/2533058/v03bt02a038-omae2017-62513.pdf.

Vasconcelos, Diogo, Mário Vieira, Diogo Dias, and Luis Reis. 2020. “Structural Evaluation of the DeepCWind Offshore Wind Platform.” *Frattura Ed Integrita Strutturale* 14 (51): 24–44. https://doi.org/10.3221/IGF-ESIS.51.03.